

Cluster interactions for fcc-based structures in the Al-Mg-Si system

Nils Sandberg¹, Mattias Slabanja² and Randi Holmestad¹

¹ *Department of Physics,*

Norwegian University of Science and Technology (NTNU)

N-7491 Trondheim, Norway

² *Department of Applied Physics,*

Chalmers University of Technology

S-412 96 Gothenburg, Sweden

(Dated: October 29, 2018)

A class of proposed coherent precipitate structures (Guinier-Preston zones) in the Al-Mg-Si alloy are investigated using first-principles density functional theory methods. The cluster expansion method is used to extract effective interaction parameters, providing the means for large scale energy calculations of alloy structures. The Mg_1Si_1 $L1_0$ structure and structures related to the Mg_5Si_6 β'' phase are studied in more detail, and e.g., precipitate/matrix interface energies are presented. Using direct first-principles calculations we show that the former phase is dynamically unstable and thus must be stabilized by the surrounding Al matrix. Monte Carlo simulations and free-energy techniques are used to study the Al rich side of the phase diagram with the current CE parameters, and kinetic Monte Carlo simulations are used to study clustering in the disordered phase. The implications of our findings are discussed in the framework of classical nucleation theories, and we outline possible nucleation mechanisms.

I. INTRODUCTION

The formation of solute-rich precipitates in a super-saturated solid solution is a process of great technological importance because it gives raise to precipitation hardening in a wide class of alloys. Among the precipitation hardened Al alloys, the Al-Mg-Si (6xxx) alloys belong to the most studied with regards to their precipitation sequences, see Ref. 1, 2, 3 and references therein. They often display a complex sequence of metastable phases forming under different conditions (time, temperature and composition). The structures of almost all of these phases are known in detail from transmission electron microscopy (TEM) studies. However, such techniques give no direct information about the energetics of the phases of interest. First-principles calculations can provide vital new information in this respect, as has recently been demonstrated in the case of the Al-Mg-Si system, see work by Derlet *et al*[4] and Ravi and Wolverton.[5] Thus, by means of solving the Schrödinger equation within the density functional theory (DFT), one can obtain enthalpies, and study relaxation and binding, in phases which are meta-stable and only exist as nano-sized particles within the host matrix. A limitation of direct first-principles calculations is that, in practice, the structure has to be specified in advance. A central and unresolved question in the case of the Al-Mg-Si system is the structure of the first precipitates that form from solid solution, i.e., the Guinier-Preston (GP) zones.[3]

In order to be able to study coherent precipitate phases within the Al matrix, and to model the disordered phase and the nucleation process, we have utilized a ternary cluster expansion (CE) description of the Al-Mg-Si system. In this model, a set of atoms within a lattice structure is denoted by σ , and the total energy of such a configuration can be written as a sum of “cluster functions”,

$$\Phi_{\alpha,s}(\sigma);$$

$$E(\sigma) = E_0 + \sum_{\alpha,s} V_{\alpha,s} \Phi_{\alpha,s}(\sigma). \quad (1)$$

We derive the cluster interaction parameters $V_{\alpha,s}$ from a set of first-principles calculations using an approach based on the structure inversion method (SIM).[6] Once these parameters have been obtained, it is a relatively inexpensive operation to sum up the total energy. A complication that arises is that the effective cluster interactions are in principle volume dependent,[7] but since the concentration of Mg and Si in typical Al-Mg-Si alloys is 1 – 2%, we have done all calculations at volumes corresponding to the Al equilibrium lattice constant.

We have focused on the two main candidates for early precipitate structures, or GP-zones, in the Al-Mg-Si system. These are, the Mg_1Si_1 $L1_0$ structure proposed by Matsuda *et al*.[8] here referred to as the Matsuda structure, and the so called pre- β'' -phase which was proposed by Marioara *et al*.[9] By testing a large number of structures related to the pre- β'' structure, we conclude that the Matsuda-phase is the energetically most stable precipitate phase. We then proceed with studying the stability of the Matsuda and pre- β'' structures and find that the former structure is dynamically unstable, so that the vibrational free energy is undefined. This implies that it can only exist within a surrounding stabilizing lattice, the Al lattice in this case. That this system exhibits instabilities is not surprising since fcc Si is dynamically unstable.[10] For certain local concentrations of Si we therefore expect the lattice to be significantly softened, which lowers the Gibbs free energy, and may lead to structural transformations.

The CE method also allows for large-scale Monte Carlo (MC) simulations to be performed, either for finding ground-state structures (using, e.g., simulated annealing)

or to study finite-temperature thermodynamic properties of an alloy. Our MC calculations using the present CE parameters show that decomposition typically occurs in the form of spherical precipitates with the Matsuda structure. MC simulations in combination with thermodynamic integration are used to calculate the solvus phase boundary in the Al rich end of the phase diagram. We also use kinetic Monte Carlo (kMC) simulations to study clustering in the disordered phase. Such studies are of current interest because modern experimental techniques, i.e., high-resolution transmission electron microscopy and 3D atom probe tomography, are capable of studying small, coherent clusters at an atomic scale.[3, 11] Therefore, increased understanding of atomic level processes that precede nucleation can be expected and a much more detailed comparison with modelling and simulation is possible.[11]

The paper is disposed as follows. In Sec. II we describe the two GP-zone models considered in this work. In Sec. III we review the theory of ternary CE, and we also detail the first-principles calculations that form the basis for the present work. The results of the fitting procedure, and of the CE calculations for different GP-zone structures are presented in section IV. The calculation of the solvus boundary for Mg_1Si_1 and simulations of the early stage of clustering are presented in the same section. In Sec. V we discuss the present results in the light of what is experimentally known about GP-zone formation in Al-Mg-Si, and conclusions follow in Sec. VI.

II. GP-ZONE MODELS IN THE AL-MG-SI ALLOYS

Currently there are two generally accepted models of the early precipitate phases, or GP-zones, in the Al-Mg-Si alloys. The first structure, an Mg_1Si_1 L1₀ phase (see Fig 1b) was observed by Matsuda and co-workers [8] in samples with a solute concentration of 1.55 at.% and with a Mg:Si ratio of 2:1. The samples had been aged and then heat-treated at 343 K. This phase will be referred to as the Matsuda phase. The other structure, the pre- β'' in Fig. 1a was proposed by Marioara et al. [9] based on TEM observations of samples that had been homogenized at 843 K and heat treated at 450 K. The Mg:Si ratio in these samples was 5:6.

The β'' structure is the most efficient hardening phase in the 6xxx alloys. The fact that GP-zones have been observed to have the same symmetry as the β'' phase, motivated the structural model of GP-zones shown in Fig. 1a.[9] Its structural relationship with the β'' phase can be understood in the following way. If the $(0, 0, 0)$ Mg atom in Fig. 1a is displaced $1/2a_0$ in the normal (z) direction, one obtains a structural model of the β'' phase. The latter phase is in turn needle-shaped, and often observed to be coherent in the (x, y) plane and semi-coherent in the z (needle) direction.

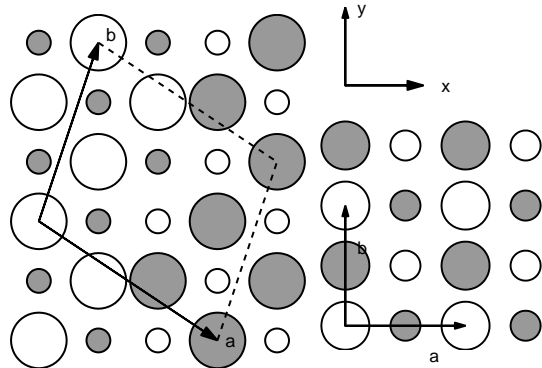


FIG. 1: Previously proposed GP-zone structures, where large (small) circles indicate Mg (Si) atoms. Dark atoms are displaced by $1/2 a_0$ in the z -direction, with respect to the white atoms. a) the pre- β'' structure with composition Mg_5Si_6 , the 11 atom primitive unit cell is indicated. b) the Matsuda L1₀ structure with composition Mg_1Si_1 .

III. METHODS

A. Cluster expansion and the structure inversion method

The general theory for multicomponent CE was developed by Sanches, Ducastelle and Gratias.[12] In the present work we use the following notations. A lattice site i can be occupied by an atom of type A , B , or C , indicated by an occupation variable, σ_i , taking the value -1 , 0 , or $+1$, respectively. Hence, given an underlying lattice, the alloy structure can be defined by a set of occupation variables, $\sigma = \{\sigma_i\}$. Linearly independent basis vectors describing the occupation are then

$$\begin{aligned}\Theta_i^{(0)} &= 1, \\ \Theta_i^{(1)} &= \sqrt{3/2}\sigma_i, \\ \Theta_i^{(2)} &= \sqrt{2}(1 - 3\sigma_i^2).\end{aligned}\quad (2)$$

A cluster α is defined as a set of lattice sites (p_1, p_2, \dots, p_n) . Given a cluster α , a cluster function is defined as the the product of the basis vectors,

$$\Phi_{\alpha,s}(\sigma) = \Theta_{p_1}^{(s_1)}\Theta_{p_2}^{(s_2)}, \dots \quad (3)$$

where the sequence $s = (s_1, s_2, \dots, s_n)$ is called “decoration”, which in the ternary case will consist of 1:s and 2:s. The total energy is given by (1), and by considering the average of cluster functions for symmetry-equivalent cluster-decoration pairs, $\bar{\Phi}_{\alpha,s}(\sigma)$, the total energy can be re-written as

$$E(\sigma) = E_0 + \sum_{\alpha,s} V_{\alpha,s} m_{\alpha,s} \bar{\Phi}_{\alpha,s}(\sigma), \quad (4)$$

where E_0 is a reference energy and $\bar{\Phi}_{\alpha,s}(\boldsymbol{\sigma})$ is an average, defined as

$$\bar{\Phi}_{\alpha,s}(\boldsymbol{\sigma}) = \frac{1}{N} \sum_{\alpha',s'} \Phi_{\alpha',s'}(\boldsymbol{\sigma}). \quad (5)$$

The sum goes over all (α',s') pairs related to (α,s) through lattice symmetry operations. $m_{\alpha,s}$ is the number of such cluster functions per lattice site, and N is the total number of lattice sites.

In the structure inversion method one calculates the $V_{\alpha,s}$ by minimizing

$$\omega = \frac{1}{n} \sum_{\{\boldsymbol{\sigma}\}} [E_{\text{DFT}}(\boldsymbol{\sigma}) - \sum m_{\alpha,s} V_{\alpha,s} \hat{\Phi}_{\alpha,s}(\boldsymbol{\sigma})]^2 \quad (6)$$

where $\{\boldsymbol{\sigma}\}$ denotes a list of n input structures and $E_{\text{DFT}}(\boldsymbol{\sigma})$ their corresponding total energies. The choice of input structures is arbitrary as long as they contain information about all cluster functions, and an advantage with the SIM is that the $\boldsymbol{\sigma}$:s can consist of small unit cells in a super-cell approach, for which the total energy, may be efficiently calculated using DFT methods.

In order to select cluster functions to be used in the fitting, we used cross-validation,[13] with the intention to obtain an optimal fit, while at the same time avoid over-fitting. It is applied to CE by defining a hierarchy of clusters, where a cluster is included only if all its sub-clusters are included, and short range clusters are prioritized over long-range clusters. Then, by choosing clusters in this way, the aim is to minimize the cross-validation score

$$(cv)^2 = \frac{1}{n} \sum_{i=1}^n (E_i - E_{(i)})^2. \quad (7)$$

Here, $E_{(i)}$ denotes the predicted energy of structure i , using parameters $V_{\alpha,s}$ obtained *without* structure i included in the fit. Thus, the cv-score measures the ability of the CE, with a given set of cluster functions, to predict the energy of new structures. We note that all n structures are included in the fit in Eq. (6).

B. Electronic structure calculations

We have used the Vienna ab-initio simulation package (VASP),[14] a plane-wave pseudo potential implementation of the DFT method, in the present electronic structure calculations. For the exchange-correlation approximation we used the Perdew-Wang implementation of the generalized gradient approximation (GGA).[15] The built-in ultra-soft pseudo potentials by Vanderbilt *et al.* were used.[16] k -points were chosen according to the Monkhorst-Pack scheme in meshes corresponding to $12 \times 12 \times 12$ points for the conventional fcc unit cell, or denser. Tests showed that using a mesh corresponding to $16 \times 16 \times 16$ k -points changed the energy with typically 1-2 meV/atom. The atomic structure was relaxed at

constant volume using a conjugate gradient technique, or in some cases a damped molecular dynamics algorithm. We found that both methods led to the same relaxed state. We note that during the relaxation, the symmetry is preserved. This means that if the relaxation starts at a saddle point in the potential energy landscape, the system may stay at this saddle point due to symmetry restrictions. In particular, pure Si in the fcc structure is unstable with respect to tetragonal shear,[10] but this relaxation mode is not taken into account in our calculations.

C. Monte Carlo and kinetic Monte Carlo simulations

The computational study of the thermodynamic properties of the Al-Mg-Si system requires to take configurational space properly into account. To this end we use the standard Metropolis[17] Monte Carlo sampling technique, generating a sequence of configurations being Boltzmann-distributed with respect to the system temperature and configurational energy. We have held the alloy constituent concentrations unchanged during the simulations. Hence, as the trial-changes we simply choose a random pair of atoms to be exchanged with each-other. One MC step is defined as one such trial-exchange per atom. A technical aspect of our implementation is that the cluster functions are defined in the so called canonical basis rather than the orthogonal basis (Eq:s (2)). That means that the cluster functions are products of integers rather than real numbers, and their evaluation becomes more efficient.

In order to simulate kinetic processes (e.g., nucleation) we have utilized a kinetic Monte Carlo (kMC) algorithm. The important additional constraint added to a kMC algorithm, as compared to the ordinary MC dito, is that the (trial-) changes made to the system are selected in a way corresponding to the effect of some physical process occurring. The physical process being most important during aging or phase transformations in our Al-Mg-Si alloy system, is the mass transport via atomic diffusion. The atomic diffusion process was modelled by attempted interchange of two randomly chosen nearest neighbor atoms, and accepting the interchange according to the Metropolis algorithm. This model is also known as Kawasaki-dynamics.[18]

To provide an estimate of the time-scale of the simulated diffusion process, we use an experimental value of the aluminum self diffusion coefficient[19] as input. The experimental input which implicitly contain information about diffusion hop-rates and vacancy concentrations, will relate the Monte Carlo steps to physical time as

$$\tau(T) \sim \frac{a_0^2}{D_{\text{exp}}(T)} \frac{1}{s_v}, \quad (8)$$

where τ is the physical time scale of giving all the atoms

in the system a chance to diffuse, a_0 being the Al lattice constant, and $D_{\text{exp}}(T)$ is the experimentally determined diffusion coefficient. The factor s_v accounts for the supersaturation of vacancies that is present, e.g., after a quench.

We used the kMC method to study the early stage of clustering in Al-Mg-Si. Our definition of a cluster is then that each solute atom (Mg or Si) belonging to a given cluster is nearest neighbour to at least one more solute atom in the same cluster.

D. Free energy integration

The phase diagram, and the underlying free-energy differences between various phases determine the driving force, e.g., for precipitate formation. In order to calculate the phase boundary between disordered and a two-phase region, one must know the free energy of the disordered phase. In the present work, it was calculated in the following way. The energy as a function of temperature was determined for a set of compositions in standard MC simulations. This was done by slowly decreasing the temperature and the system was then kept in the disordered state. A corresponding simulation where the temperature is increased from a low temperature shows a clear hysteresis and the point where the two curves meet can be taken as a rough estimate of the phase boundary. The entropy in the disordered state was determined using thermodynamic integration of the relation

$$\frac{dS}{dT} = \frac{1}{T} \frac{dH}{dT}. \quad (9)$$

The remaining constant of integration was taken from the expression for the entropy of a ternary system in the ideal solution model

$$S_{\text{ideal}} = -k_B(c_1 \ln(c_1) + c_2 \ln(c_2) + c_3 \ln(c_3)) \quad (10)$$

where c_1 , c_2 and c_3 are the respective atomic concentrations. This expression is which is valid at sufficiently high temperature. In the present work, we integrated from $T = 3000$ K.

IV. RESULTS

A. Fitting of the CE parameters

To choose input structures for the SIM, we started with 8 binary structures and 34 ternary structures in Refs. 20 and 21, respectively. Those structures have been shown to be the only distinct structures that can be obtained if one assumes only up to next-nearest neighbor pair interactions. (In the ternary case, this has not been strictly proven, but it seems plausible.) Taking into account the structures obtained when the occupation of A, B or C atoms in the 'generic' structures are permuted, one ends

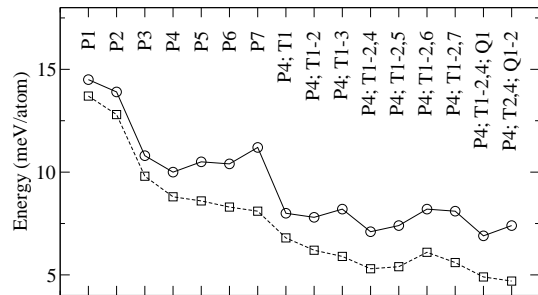


FIG. 2: Convergence of the cv-score (circles) and the mean-square deviation between predicted and calculated energies of the input structures (squares), as a function of included clusters; pairs (P), three-point clusters (T), and four-point clusters (Q). It is understood that, e.g., P4 means P1-4. See further Table 1.

up with 148 symmetrically distinct structures. In addition, we used some low-concentration structures, e.g., an isolated impurity in a 32 LP cell, see Appendix A. Further, we excluded some structures, e.g., pure Mg, that had a large static (positive or negative) internal pressure. In total, we ended up with 154 structures.

These structures were used as input to the fitting of the cluster interaction parameters in Eq. (6). When selecting clusters, we minimized the cross-validation score given by Eq. (7). In the procedure we included pairs, triplets and quadruplets in a hierarchical order, see Fig. 2 and Table I for an explanation of the clusters used. We found that a good fit was obtained if we included pairs up to fourth nearest neighbor, and the triplets T1, T2 and T4 (see Table I). This gives a total of 27 parameters $V_{\alpha,s}$ that were minimized. The resulting cv-score is $cv = 7.1$ meV/atom.

B. Static energies of suggested GP-zone structures

We have investigated the energetics of two models of the GP-zones in Al-Mg-Si; the Matsuda phase and the pre- β'' phase (see Sec. II and Fig. 1).

Because the latter structure has not actually been solved, we proceed along the lines in Ref. 5: starting with the 11 atom unit cell in Fig. 1a, we exchanged Mg/Si atoms with Al atoms in all $2^{11} = 2048$ possible ways. For each structure (of which some will be identical by symmetry) we calculated the total energy using Eq. (1). In Fig. 3 we have plotted, for each composition $c_{\text{Mg}}/(c_{\text{Mg}} + c_{\text{Si}})$, the energy of the most stable structure. An even less restrictive procedure is to generate all $3^{11} = 177147$ structures that arise if each lattice point is occupied by a Al, Mg or Si atom. The most stable structures in this case are essentially the same as those in Fig. 3.

Ravi and Wolverton[5] did a set of calculations for pre- β'' structures, using first-principles methods. We have used the same convention as they used in plotting the energies, i.e., we plot the formation energies per solute

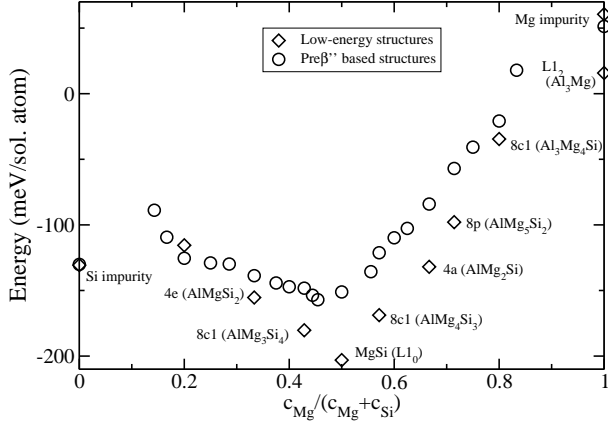


FIG. 3: Total energy per solute atom of different suggested GP-zone structures, along with some of the structures used in the fitting procedure. The results are given with reference to the energies of the pure elements, in the fcc structure, at zero pressure. The structures marked with diamonds are denoted in accordance with Ref. 21.

atom with respect to the pure constituents in the fcc structure. Therefore, the the two sets of energies can be directly compared.

Fig. 3 shows that structures with an Mg:Si composition close to 1:1 are energetically favoured. This is in line with most experimental data on clusters and early precipitates in Al-Mg-Si alloys.[8] For this composition, the Matsuda phase is lowest in energy, as found also in Ref. 5. In order to picture how “pre- β'' -like” structures may be build up, we also extracted the energetically most stable structures contained in the pre- β'' cell as a function of solute concentration $c_{\text{sol}} \equiv c_{\text{Mg}} + c_{\text{Si}} = 1/11, \dots, 11/11$. Selecting the structures from the 2^{11} or the 3^{11} possible structures resulted in the same ground state structures. The energies are plotted in Fig. 4 together with directly calculated energies for the same structures. Thus, by comparing the two sets of energies, one gets an estimate of the predictive power of the CE method used. We note the the relaxation of the structure at $c_{\text{sol}} = 9/11$ did not finish during the simulation. This could indicate that the structure is unstable. Some representative lowest-energy structures in Fig. 4 are shown in Appendix B.

The interface energies between secondary phase particles and a parent phase are important parameters in various theories of nucleation and phase stability that are usually hard to estimate. We calculated the pre- β'' /Al and Matsuda/Al interface energies (at $T = 0$) using Eq. (1), see Table II. The finding that the pre- β'' /Al ($\bar{3} 1 0$) interface is negative was confirmed in a direct DFT calculation in a 44 atom super-cell. The result indicates that this phase may contain Al.

The energy $E(\sigma)$ of Eq. (4) is the static energy at constant volume. To this comes a lowering of elastic energy, ΔE^{elast} , due to volume and cell-shape relaxation of these phases. For the structures that were used in the fitting

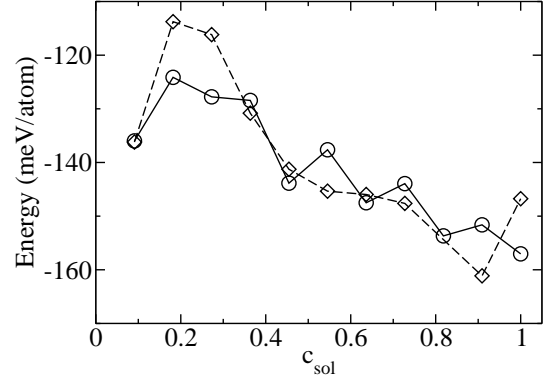


FIG. 4: Predicted ground state structures in the 11 atom unit cell of the pre- β'' structure (circles) as a function of solute concentration. Diamonds indicate the total energies obtained in direct DFT calculations for the same structures.

of the CE parameters, this term can be estimated in the following way. Assuming that the phase B relaxes centrosymmetrically within an A matrix, which is assumed to be elastically isotropic, ΔE^{elast} is given by[22]

$$\Delta E^{\text{elast}} = 18\mu_A K_B / (3K_B + 4\mu_A) \epsilon^2 v_B \quad (11)$$

Here, μ_A is the shear modulus of the A phase and K_B is the bulk modulus of the B phase, where in this estimate we used $K_{\text{Si, fcc}} = K_{\text{Al}}$. v_B is the volume of B phase and ϵ is the initial linear misfit of the B phase relative to the A phase. ϵ is in turn calculated from the internal pressure p of the different structures using $V_0 = V / (1 - p/K)$. The results for some structures in Fig. 4 are given in Table III.

C. Dynamical stability of the Matsuda and pre- β'' phases

The dynamic stability of the Matsuda phase and the pre- β'' phase was tested by displacing the atoms from their relaxed positions in the internally relaxed structures. For the Matsuda phase, starting with a 32 atom cell, we displaced the atoms in random directions $1/50$ of a nearest-neighbor distance. A subsequent relaxation showed that the forces were non-conservative (i.e., directed away from the initial positions) for the Si atoms within the Si plane.

A similar analysis of the pre- β'' structure shows that it is most likely metastable. In a separate calculation, we displaced the $(0, 0, 0)$ Mg atom in Fig. 1a by a small distance in the z -direction. Also in this case, the force on the Mg atom was conservative.

In the case if the Matsuda phase, we note that, according to the findings in Ref. 8, the structure exists in thin (one or a few atomic) $(0 1 0)$ slabs in the Al lattice (see Fig. 1b). For such morphologies, the Matsuda phase will be stabilized by the surrounding Al lattice.

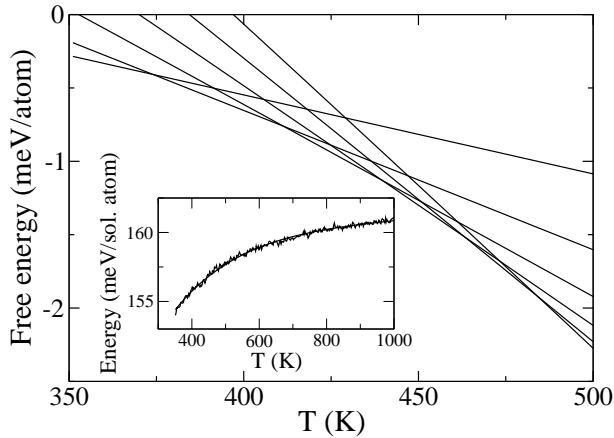


FIG. 5: Free energies for the disordered phase, calculated by thermodynamic integration from a reference state at 3000 K. The lines correspond to $c_{\text{sol}} = 1, 2, \dots, 6$ at.% solutes, in order of increasing slope. The zero energy correspond to the reference state of completely separated $L1_0$ and Al phases, $E = c_{\text{sol}}E_{\text{Al}} + (1 - c_{\text{sol}})E_{L1_0}$. The inset shows one of the switching runs, at $c_{\text{sol}} = 2\%$. The polynomial fit is included, and overlaps with the energy points.

D. Free energy of precipitation and kinetics of clustering

In order to study precipitation and clustering it is necessary to know the solubility limit of the alloying elements. In this sub-section we first describe the calculation of the solvus boundary in the Al rich end of the phase diagram, and then we present kMC simulations of clustering in the disordered phase.

We have focused on the subset of the phase diagram where the Mg:Si ratio is 1:1 and $c_{\text{sol}} = c_{\text{Mg}} + c_{\text{Si}}$ varies between 0 and 5 %. The energy per atom as a function of T was calculated for a range of concentrations, while staying in the disordered phase. In these simulations, an $80 \times 80 \times 80$ atom system was cooled at a rate of 0.02 K/kMC step. Based on a polynomial fit to the energy, we then used thermodynamic integration to calculate the entropy by use of Eqs. (9) and (10). The corresponding free energies are plotted in Fig. 5. The free energies are given with respect to the normal state, which corresponds to separated Al and $L1_0$ phases at 0 K. The solubility limit at each temperature corresponds to the lowest lying free-energy curve. We have implicitly assumed that the ordered phase, the $L1_0$, is completely ordered, i.e., does not contain anti-defects or Al atoms. We checked the validity of this assumption, again using the regular solution model. It turns out that defects (typically 1-2% below 500 K), can be neglected in the calculation of the solubility limit at the Al rich end of the phase diagram. The resulting solvus-line is plotted in Fig. 6.

Clustering in Al-Mg-Si was studied by kMC. The atoms were initially randomly distributed, correspond-

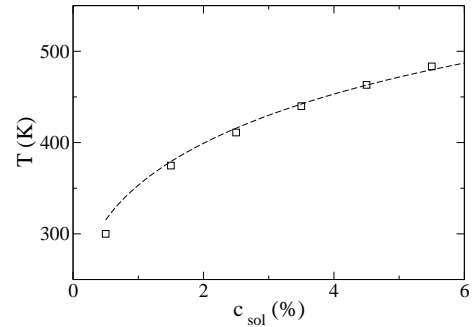


FIG. 6: Calculated solvus line dividing the disordered and the two-phase regions of the phase diagram for which $c_{\text{Mg}} = c_{\text{Si}} = c_{\text{sol}}/2$ (squares). The dashed line corresponds to an estimate based on the regular solution model.

ing to a previous homogenisation at a high temperature. In Fig. 7 we have displayed the cluster size distributions as a function of annealing time for a 2% solution at 400 K. The time-scale was calculated by assuming the Al self-diffusion rate $D_{\text{Al}} = 1.5 \times 10^{-5} \exp(-1.33/k_{\text{B}}/400)$ and a 10000-fold increase in the number of vacancies, corresponding to a homogenisation at 750 K. We believe that the latter factor is the dominant source of error in estimating the time-scale in this type of simulations. It is seen that the initial stage of clustering is fast (~ 1 min.). In practice, since the kinetics is even faster at higher T , part of the initial clustering is expected to take place already during the quench.

Since the system is not within the two-phase region, there are no nucleation and growth stages. After the initial clustering, the cluster sizes fluctuate in accordance with[23]

$$N^{\text{eq}}(i)/N = \exp(-\Delta F(i)/k_{\text{B}}T) \quad (12)$$

where $\Delta F(i)$ is the excess free energy required to form a cluster of size i , and N^{eq} is the number of such clusters in a system containing N atoms. $\Delta F(i)$ can be written as

$$\Delta F(i) = i\Delta f_{\text{vol}} + Bi^{2/3}\sigma \quad (13)$$

where Δf_{vol} is the volume free energy per atom of a cluster, σ is the cluster/matrix interface free energy and B is a geometrical factor.

A longer kMC simulation (6×10^6 kMC steps for $80 \times 80 \times 80$ atoms) showed that the cluster sizes were distributed in accordance with Eq. (12) for clusters from $i = 8$ up to $i = 16$, with an effective volume energy close to 0 and an interface energy $\sigma = 3 \text{ meV}/\text{\AA}^2$, i.e., considerably lower than the mean interface energy of the Matsuda phase at 0 K (Table II).

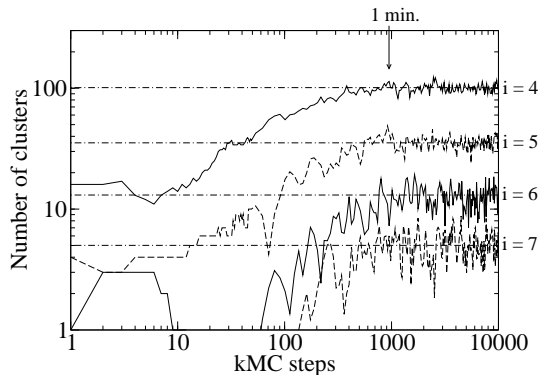


FIG. 7: Log-log plot of the number of clusters of a given size i , calculated in a kinetic Monte Carlo simulation of an $80 \times 80 \times 80$ atom system. The horizontal lines are the mean number of clusters over a total of 6×10^6 kMC steps. kMC steps have been related to physical time as described in the text.

V. DISCUSSION

The main purpose of this paper was to apply the CE-SIM method to model clusters and GP-zones in the Al-Mg-Si system. The interaction parameters $V_{\alpha,s}$ were fitted to reproduce the static energy E of fcc based structures in the low solute-concentration regime. By use of cross-validation and by selecting clusters of increasing range, we ensure that an 'optimal' set of clusters is selected in the fitting procedure. Explicit calculations on 10 predicted ground-state structures derived from the pre- β'' structure reveal that the method holds its promise; the mean square deviation between predicted and directly calculated energies is 7.25 meV/atom, to be compared with the cv-score $cv = 7.1$ meV/atom in the fitting procedure.

However, the energy of interest for a given σ is the Gibbs free energy $G = E - TS + pV$. The pV term can be handled within the CE formalism,[7] but it is much more difficult to treat the TS term in a completely general manner. Our explicit calculations for the Matsuda phase show that it is dynamically unstable, i.e., the TS term is undefined. In general, one expects that when the local configuration approaches an unstable structure, the vibrational frequencies are lowered (phonon softening), so that the structure is stabilized. Thus, this is an effect that we expect to be important in the early stages of precipitation in Al-Mg-Si. We note that in Al-Sc, the inclusion of the TS term changes the phase diagram significantly.[24] This is related to phonon softening but not to instabilities. Instabilities in substitutional alloys have been studied previously, e.g. in W-Re.[25]

We now discuss the implications of our findings in relation to what is known from experiments on the nucleation of GP-zones and the β'' -phase. In our simulations, we have only found one stable precipitate structure; the Mg_1Si_1 $L1_0$ structure. It forms in approximately spher-

ical precipitates below $T \approx 400$ K for the composition $c_{\text{Mg}} + c_{\text{Si}} = 2$ %. Matsuda et al. report the formation of Mg_1Si_1 $L1_0$ precipitates at $T = 323$ K for an alloy containing 1.6 mass % Mg_2Si . These precipitates are in the form of (0 1 0) planes. The morphology can be related to the internal stress of the Matsuda structure, which favours platelets in the (0 1 0) plane. Because the platelets extend only one or a few planes in the normal direction, the Matsuda phase will be stabilized by the surrounding Al matrix.

The pre- β'' and β'' phases are found experimentally to form at $T = 423...523$ K in alloys containing about 1.25 at.% Al and Mg.[3] Fig. 6 shows the calculated phase boundary for forming Matsuda particles. One finds that neither the Matsuda phase nor the pre- β'' phase would form with the current atomic interaction parameters, at the temperatures and solute concentration where β'' forms. Elastic relaxations would lower the energies of both the impurities and the ordered phases, and are not expected to change this conclusion (see further Ref. 5). It is seen in Fig. 6 that the regular solution model describes the solvus phase boundary well up to $c_{\text{sol}} \sim 4\%$. For a Mg:Si composition of 1:1, the expression for the solvus line according to this model is $c \approx 2 \exp(-\Delta E/k_B T)$, in the low concentration limit. ΔE is the ordering energy which can be found in Fig. 3 by comparing the energy of, e.g., the Matsuda phase with a line connecting the impurity energies of Mg and Si. Thus, one finds that the ordering energy required to stabilize a structure at the temperature and concentration where GP-zones form (≈ 450 K and 1.5% respectively), is at least 0.2 eV/atom. This is larger than any of the ordering energies in the current study or in Ref. 5.

Therefore, in order to explain the nucleation mechanism of GP-zones and the β'' phase, we suggest the following possibilities. Either, vibrational entropy effects or vacancies stabilize an ordered pre- β'' based structure, which then transforms into the β'' structure, or the structural transition takes place in the disordered phase, in a Mg-Si rich cluster with the right local configuration. Recent TEM observations clearly indicate that the GP-zones are ordered, fcc-based, structures.[3] Thus, the former explanation seems more likely. In either case, there is a substantial gain in energy connected to the transition to the β'' structure.

Finally, we remark that it is likely that quenched-in vacancies play a direct role in the nucleation of the β'' phase. As pointed out in Ref. 4, vacancies may facilitate a structural transition from the pre- β'' to the β'' phase simply by providing the extra space needed for the (0,0,0) Mg atom to move $1/2$ lattice vector in the z -direction. Including vacancies in the CE description is formally straight-forward, however, in practice it would increase the complexity in the CE and lead to other technical complications.

VI. CONCLUSIONS

We have investigated the formation of GP-zones in the Al-Mg-Si system using a CE of the total energy. DFT pseudo-potential calculations of 154 fcc-based pure, binary and ternary structures were used to parameterize the energy by the SIM. Which cluster functions to include was chosen according to the cross-validation criterion, with the intension to avoid over-fitting. The method successfully reproduces the total energy of 10 structures based on the suggested pre- β'' structure. Regarding the formation of GP-zones, the CE calculations shows that the $\text{Mg}_1\text{Si}_1\text{L1}_0$ structure suggested by Matsuda *et al.* is the most energetically stable phase. This is also confirmed in direct DFT calculations. Our results are in fair agreement with the DFT calculations presented by Ravi and Wolverton,[5] where one should compare with their *constrained* GGA results for pre- β'' structures. Re-

garding the formation of the pre- β'' and β'' structures, we outline two possible nucleation mechanisms. Either, the vibrational entropy (TS) term, or the presence of vacancies serve to stabilize the structures preceding the β'' phase, which then transforms to the meta-stable β'' phase.

VII. ACKNOWLEDGMENTS

We thank M. Ekman and C. Wolverton for helpful discussions. M. Ekman also kindly provided us with geometrical data for the CE. C. D. Marioara and S. J. Andersen contributed with their valuable knowledge about precipitation in the Al-Mg-Si system. This work was funded through the Norwegian high performance computing programme and the Norwegian reseach Council through contract nr. 140553/I30.

-
- [1] H. W. Zandbergen, S. J. Andersen, and J. Jansen, *Science* **277**, 1221 (1997).
- [2] G. A. Edwards, K. Stiller, G. L. Dunlop, and M. J. Cooper, *Acta Mater.* **46**, 3893 (1998).
- [3] C. D. Marioara, S. Andersen, H. Zandbergen, and R. Holmestad, *Met. Mater. Trans. A* **36A**, 691 (2005).
- [4] P. M. Derlet, S. J. Andersen, C. D. Marioara, and A. Frøseth, *J. Phys.: Condens. Matter* **14**, 4011 (2002).
- [5] C. Ravi and C. Wolverton, *Acta Mat.* **52**, 4213 (2004).
- [6] J. W. D. Connolly and A. R. Williams, *Phys. Rev. B* **27**, 5169 (1983).
- [7] D. B. Laks, L. G. Ferreira, S. Froyen, and A. Zunger, *Phys. Rev. B* **46**, 12587 (1992).
- [8] K. Matsuda *et al.*, *Metall. Mat. Trans. A* **29**, 1161 (1998).
- [9] C. D. Marioara, S. Andersen, J. Jansen, and H. Zandbergen, *Acta Mater.* **49**, 321 (2001).
- [10] M. Ekman, K. Persson, and G. Grimvall, *Phys. Rev. B* **62**, 14784 (2000).
- [11] G. Sha and A. Cereso, *Acta Mater.* **53**, 907 (2005).
- [12] J. M. Sanchez, F. Ducastelle, and D. Gratias, *Physica A* **128**, 334 (1984).
- [13] A. V. de Walle and G. Ceder, *J. Phase Equil.* **23**, 348 (2002).
- [14] G. Kresse and J. Hafner, *Phys. Rev. B* **47**, 558 (1993); **49**, 14251 (1994); G. Kresse and J. Furthmüller, *Phys. Rev. B* **54**, 11169 (1996).
- [15] J. P. Perdew *et al.* *Phys. Rev. B* **46**, 6671 (1992); *Phys. Rev. B* **48**, 4978 (1993).
- [16] D. Vanderbilt, *Phys. Rev. B* **41**, 7892 (1990); G. Kresse and J. Hafner, *J. Phys.: Condens. Matter* **6**, 8245 (1994).
- [17] N. Metropolis *et al.*, *Journal of Chemical Physics* **21**, 1087 (1953).
- [18] K. Kawasaki, in *Phase Transitions and Critical Phenomena*, edited by C. Domb and M. S. Green (Academic Press, New York, 1972), Vol. 2.
- [19] *Aluminum: Properties and Physical Metallurgy*, edited by J. E. Hatch (American Society for Metals, Metals Park, Ohio, 1984).
- [20] F. Ducastelle, in *Order and phase stability in alloys*, Vol. 3 of *Cohesion and structure*, edited by F. R. de Boer

TABLE I: Definition of cluster tested in the fitting procedure. In the final fit, we chose a small set of cluster with a low *cv*-score. Each decoration listed, together with the corresponding cluster α , makes up a distinct cluster function $\Phi_{\alpha,s}$.

	Cluster, α units of $(a_0/2)$	Decorations, s
Empty		
Point	(000)	1; 2
P1	(000) (110)	11; 12; 22
P2	(000) (200)	11; 12; 22
...	...	
P7	(000) (321)	11; 12; 22
T1	(000) (110) (101)	111; 211; 222
T2	(000) (011) (0 $\bar{1}$ 1)	111; 211; 121; 221; 122; 222
T3	(000) (110) ($\bar{1}$ 01)	111; 211; 121; 221; 122; 222
T4	(000) (121) (2 $\bar{1}$ $\bar{1}$)	111; 211; 221; 222
T5	(000) (211) (112)	111; 211; 121; 221; 122; 222
T6	(000) (020) (112)	111; 211; 221; 112; 212; 222
T7	(000) (110) (112)	111; 211; 121; 221; 112; 212; 122; 222
Q1	(000) (110) (101) (011)	1111; 2111; 2211; 2221; 2222
Q2	(000) (101) (011) (0 $\bar{1}$ 1)	1111; 2111; 2211; 1121; 2121; 2221; 1122; 2122; 2222

- and D. G. Pettifor (North-Holland, Amsterdam, 1991).
- [21] G. Ceder, G. Garbulsky, D. Avis, and F. Fukuda, *Phys. Rev. B* **49**, 1 (1994).
- [22] J. W. Christian, *The theory of transformations in metals and alloys* (Pergamon, Amsterdam, 2002).
- [23] F. Soisson and G. Martin, *Phys. Rev. B* **62**, 203 (2000).
- [24] V. Ozolins and M. Astra, *Phys. Rev. Lett.* **86**, 448 (2001).
- [25] M. Ekman, K. Persson, and G. Grimvall, *J. Nucl. Mater.* **278**, 273 (2000).

TABLE II: Interface energies between the Al phase and the Matsuda/pre- β phase. Energies in $\text{meV}/\text{\AA}^2$. We checked the negative value for the Al/pre- β'' ($\bar{3} 1 0$) interface in a direct DFT calculation with result given in parenthesis.

Al/pre- β''		
$(\bar{3} 1 0)$	$(2 3 0)$	$(0 0 1)$
-3.57 (-4.31)	2.44	6.44

Al/Matsuda	
$(1 0 0)$	$(0 1 0)$
12.4	5.9

TABLE III: .

Structure	pressure ($\text{meV}/\text{\AA}^3$)	Elastic energy ($\text{meV}/\text{B-phase atom}$)
	($\text{meV}/\text{\AA}^3$)	
4e (AlMgSi ₂)	-2.5777	0.0488
8c1 (AlMg ₃ Si ₄)	8.9378	0.5863
L1 ₀ (MgSi)	19.4610	2.7798
8c1 (AlMg ₄ Si ₃)	28.1928	5.8340
4a (AlMg ₂ Si)	35.4267	9.2119
L1 ₂ (Al ₃ Mg)	32.1312	7.5778

APPENDIX A: INPUT STRUCTURES

APPENDIX B: PRE- β'' -BASED STRUCTURES

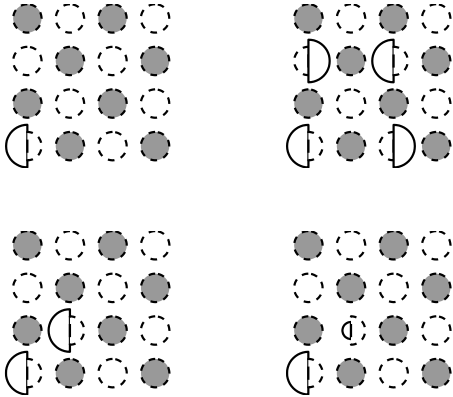


FIG. 8: 32 atom structures included in the fitting procedure. Dashed rings represent Al atoms, and oversized/undersized rings represent Mg/Si atoms. New structures obtained by interchanging Mg and Si atoms were also included. Grey atoms are situated $a_0/2$ above the white atoms. Half-circles indicate that two elements take up every second site in the vertical direction.

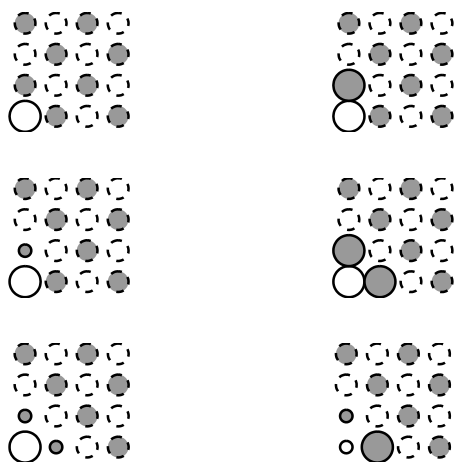


FIG. 9: 16 atom structures included in the fit. See further caption of Fig. 8.

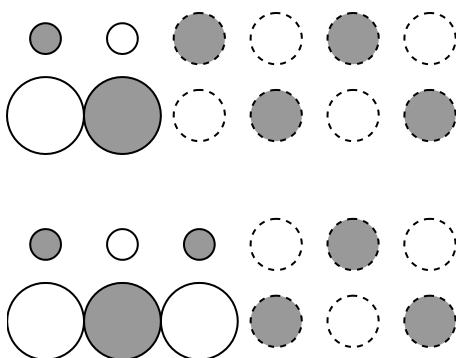


FIG. 10: 12 atom structures included in the fit. See further caption of Fig. 8.

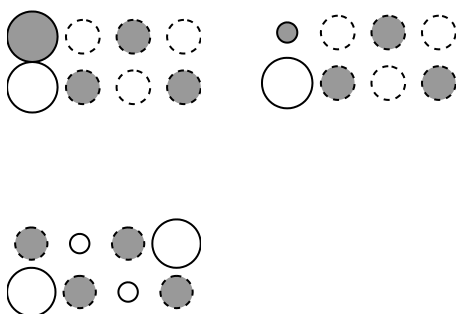


FIG. 11: 8 atom structures included in the fit. See further caption of Fig. 8.

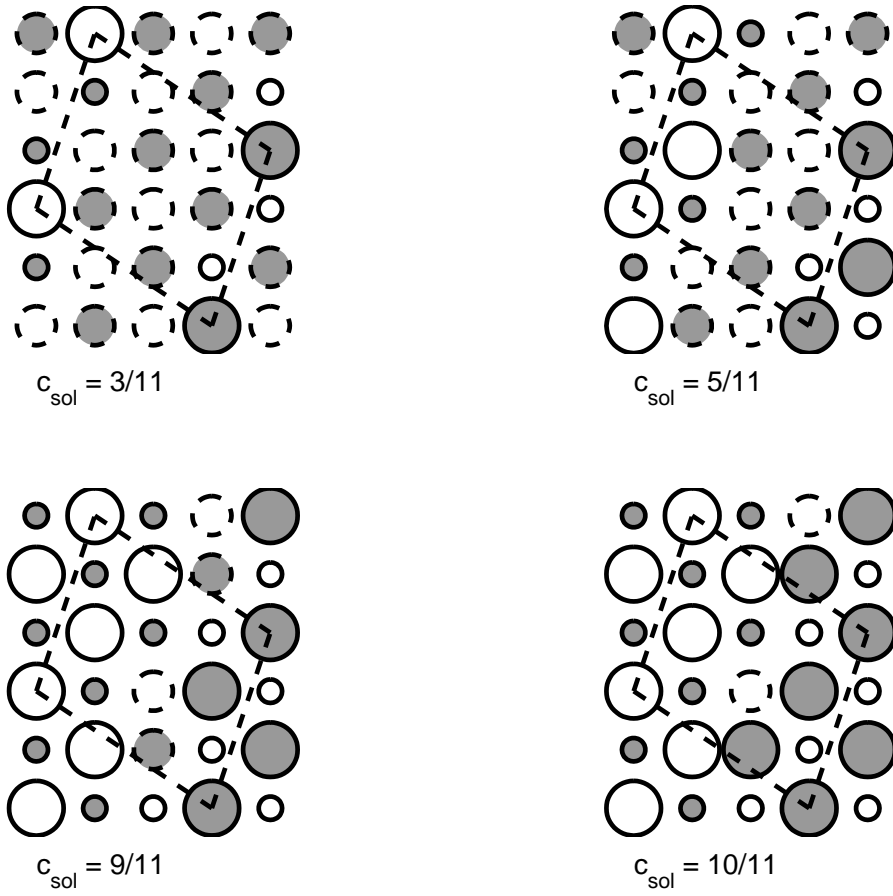


FIG. 12: Some low-energy structures based on the pre- β'' structure. See further Fig. 4.